

# The extremely high energy neutrino search with IceCube

Keiichi Mase\*, Aya Ishihara\* and Shigeru Yoshida\* for the IceCube Collaboration<sup>†</sup>

\*The department of Physics, Chiba University, Yayoi-tyo 1-33, Inage-ku, Chiba city, Chiba 263-8522, Japan

<sup>†</sup>See the special section of these proceedings

**Abstract.** A search for extremely high energy (EHE) cosmogenic neutrinos has been performed with IceCube. An understanding of high-energy atmospheric muon backgrounds that have a large uncertainty is the key for this search. We constructed an empirical high-energy background model. Extensive comparisons of the empirical model with the observational data in the background dominated region were performed, and the empirical model describes the observed atmospheric muon backgrounds properly. We report the results based on the data collected in 2007 with the 22 string configuration of IceCube. Since no event was found after the search for the EHE neutrinos, a preliminary upper limit on an  $E^{-2}$  flux of  $E^2\phi_{\nu_e+\nu_\mu+\nu_\tau} \leq 5.6 \times 10^{-7} \text{ GeV cm}^{-2} \text{ s}^{-1} \text{ sr}^{-1}$  (90% C.L.) is placed in the energy range  $10^{7.5} < E_\nu < 10^{10.6} \text{ GeV}$ .

**Keywords:** neutrinos, IceCube, extremely high energy

## I. INTRODUCTION

Extremely high energy cosmic-rays (EHECRs) with energies above  $10^{11} \text{ GeV}$  are observed by several experiments. Although there is an indication that EHECRs are associated with the matter profile of the universe [1], their origin is still unknown. The detection of cosmogenic EHE neutrino signals with energies greater than  $10^7 \text{ GeV}$  can shed light on their origin. The cosmogenic neutrinos [2] produced by the GZK mechanism [3] carry information on the EHECR source evolution and the maximum energy of EHECRs at their production site [4]. Thus, EHE neutrinos can provide fundamental information about how and where the EHECRs are produced.

The detection of EHE neutrinos has been an experimental challenge because the very small intensities of expected EHE neutrino fluxes require a huge effective detection volume. The IceCube neutrino observatory, currently under construction at the geographic South Pole, provides a rare opportunity to overcome this difficulty with a large instrumental volume of  $1 \text{ km}^3$ .

The backgrounds for the EHE neutrino signals are atmospheric muons. The large amount of atmospheric muons come vertically, while the signal comes primarily from zenith angles close to the horizon, reflecting competitive processes of generation of energetic secondary leptons reachable to a detector and absorption of neutrinos due to an increase of the cross-sections. The atmospheric muon backgrounds drop off rapidly with

increasing energy. Therefore, a possible EHE neutrino flux will exceed the background in the EHE region ( $\gtrsim 10^8 \text{ GeV}$ ). The signal is separated from the backgrounds by using angle and energy information.

## II. THE EHE EVENTS AND THE ICECUBE DETECTOR

At extremely high energies, neutrinos are mainly detected via secondary muons and taus induced during the propagation of EHE neutrinos in the earth [5]. These particles are seen in the detector as a series of energetic cascades from radiative energy loss processes such as pair creation, bremsstrahlung and photonuclear interactions rather than as minimum ionizing particles. These radiative energy losses are approximately proportional to the energies of the muon and tau, making it possible to estimate its energy by observing the energy deposit in the detector.

The Cherenkov light from the particles generated through the radiative processes are observed by an array of Digital Optical Modules (DOMs) which digitize the charges amplified by the enclosed 10" Hamamatsu photomultiplier tubes (PMTs) with a gain of  $\sim 10^7$ . The total number of photo-electrons (NPE) detected by all DOMs is used to estimate the energy of particles in this analysis. It is found that NPE is a robust parameter for estimating the particle energy.

The data used in this analysis were taken with the 22 string configuration of IceCube (IC22). Each string consists of 60 DOMs and 1320 DOMs in total with 22 strings. The data taking began May, 2007, and continued to April, 2008. This analysis used a specific filtered data to select high energy events, which requires a minimum number of 80 triggered DOMs. The total livetime is 242.1 days after removing data taken with unstable operation. The event rate at this stage is  $\sim 1.5 \text{ Hz}$  with a 16% yearly variation. Then, 6516 events with NPE greater than  $10^4$  (corresponding to CR primary energy of about  $10^7 \text{ GeV}$  and neutrino energy of about  $10^6 \text{ GeV}$  (with  $E^{-2}$  flux)) are selected and used for the further analysis.

## III. BACKGROUND MODELING

### A. Construction of the empirical model

Bundles of muons produced in CR air showers are the major background for the EHE signal search. Multiple muon tracks with a small geometrical separation resemble a single high energy muon for the IceCube detector. An understanding of the high energy atmospheric muon backgrounds is essential for the EHE signal search.

However, the backgrounds at the relevant energy range ( $> 10^7$  GeV) is highly uncertain because of the poorly characterized hadronic interactions and composition of the primary CR where no direct measurement is available.

Therefore, we constructed an empirical model based on the Elbert model [6], optimizing the model to match the observational data reasonably in the background dominant energy region ( $10^4 < \text{NPE} < 10^5$ ). The model is then extrapolated to higher energies to estimate the background in the EHE signal region. (See Fig. 1)

The original Elbert model gives a number of muons for a CR primary energy  $E_0$  such as

$$N_\mu = \frac{E_T}{E_0} \frac{A^2}{\cos \theta'} \left( \frac{AE^\mu}{E_0} \right)^{-\alpha} \left( 1 - \frac{AE^\mu}{E_0} \right)^\beta, \quad (1)$$

where  $A$  is the mass number of primary CRs with energy of  $E_0$ , and  $\theta'$  is the zenith angle of a muon bundle.  $\alpha$ ,  $\beta$  and  $E_T$  are empirical parameters. The energy weighted integration of the formula relates the total energy carried by a muon bundle  $E_\mu^{B,surf}$  to the primary CR energy  $E_0$  as,

$$\begin{aligned} E_\mu^{B,surf} &\equiv \int_{E_{th}^{surf}}^{E_0/A} \frac{dN_\mu}{dE_\mu} E_\mu dE_\mu \\ &\simeq E_T \frac{A}{\cos \theta'} \frac{\alpha}{\alpha - 1} \left( \frac{AE_{th}^{surf}}{E_0} \right)^{-\alpha+1} \end{aligned} \quad (2)$$

where  $E_{th}^{surf}$  is a threshold energy of muons contributing to a bundle at surface and depends on the zenith angle. A surface threshold is related to a threshold energy at the IceCube depth  $E_{th}^{in-ice}$ , by assuming a proportional energy loss to the bundle energy during propagation. This threshold at the IceCube depth is independent of zenith angle.

With help of a Monte-Carlo (MC) simulation for the detector response as well as the measured CR flux, it is possible to predict the NPE distribution for certain  $\alpha$  and  $E_{th}^{in-ice}$  parameters. The CR flux used in this analysis is taken from the compilation of several experimental observations in Ref. [7]. The detector response including the Cherenkov photon emission, the propagation in the detector volume and the PMT/DOM response is simulated with the IceCube simulation program. The  $\alpha$  and  $E_{th}^{in-ice}$  parameters are, then, optimized to express the observed NPE distributions. The best optimized parameters are derived as  $\alpha = 1.97$  and  $E_{th}^{in-ice} = 1500$  GeV.

With this empirical model, a simple simulation is feasible rather than simulating all muon tracks in a bundle, where the multiplicity can reach ten thousand for CR primary energies of  $10^{11}$  GeV. Therefore, a bundle is replaced by a single track with the same energy as the entire bundle. It is shown in the next section that this substitution works well to express the observational data.

Data generated with CORSIKA [8] (with the SIBYLL high energy hadronic interaction model) are also used.

However, the extensive resources required for MC generation precludes production of MC data with energy above  $10^{10}$  GeV. Therefore, the CORSIKA data are mainly used to confirm the empirical model in the background dominant energy region and provide redundant tools to study systematic uncertainty on the background estimation.

The relation between CR primary energy and the NPE (which is the empirical model itself) is independently verified by using information from coincident events with the in-ice and surface detectors. The surface detectors can estimate the CR primary energy and the in-ice detectors give NPE. The relation is found to be consistent with the empirical model we derived.

### B. Comparison between observational data and MC

An extensive comparison between the empirical model and the observational data was performed. The empirical model is found to describe the observational data reasonably in most cases. However, a significant difference was found in the  $z$  position (depth) of the center of gravity of the event (CoGZ) distribution. Many events are found in the deep part of the detector for the empirical model, while the events concentrate more at the top for the observational data. The difference is only seen for the vertical muons. This is probably due to the simple single muon substitution for the muon bundles in the empirical model. The more energetic single muons penetrate into the deep part, while many low energy muons in the bundles lose energies at the top of the detector for the vertical case. However, for the inclined cases, the bundles are already attenuated before coming to the detector, giving reasonable agreement between the observational data and the empirical model. Therefore, vertical events whose reconstructed zenith angles are less than  $37^\circ$  are not used in this analysis. A simple algorithm is used for the angle reconstruction, based on the time sequence of the first pulses recorded by DOMs.

Several distributions for the observational data and MC data after removing the vertical events are shown in Fig. 1 as well as the expected GZK cosmogenic neutrino signal [4]. As seen in the figure, the empirical model describes the observational data reasonably. The observed CoGZ distribution is also well represented by the empirical model after removing vertical events. The observed data are bracketed by the pure CORSIKA (SIBYLL) proton and iron simulation as expected.

Some up-going events are seen in the observational data, though this is consistent with the empirical background model. It is found that they are horizontally misreconstructed. On the other hand, fewer horizontal events are found for the CORSIKA data sets. This is because the CORSIKA data exhibit a better angular resolution of  $1.4^\circ$  (one sigma) compared to the empirical model of  $2.5^\circ$ . The angular resolution for the observational data is estimated with help of the IceTop geometrical reconstruction. The estimated resolution is  $2.5^\circ$  and consistent with the one of the empirical model. Another difference

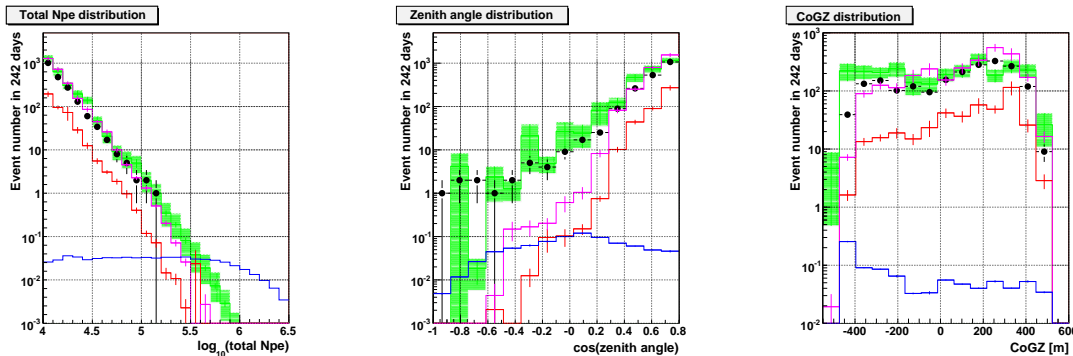


Fig. 1. The total NPE, zenith angle and CoGZ distributions between observational and MC data. The black dots represents observational data, green lines for empirical model (The shade expresses the uncertainty of the model), red for proton (CORSIKA, SIBYLL) and magenta for iron (CORSIKA, SIBYLL). The expected signal from GZK neutrinos[4] is also plotted with blue lines.

between the observational data and the CORSIKA data is found in the CoGZ distribution. The CORSIKA data concentrate more at the top of the detector especially for vertical events. The CORSIKA data also show a narrower distribution in the relation of CR primary energy and the NPE. All these facts seem to indicate that the bundles in CORSIKA consist of more lower energy muon tracks compared to the observational data, leading to bundles with less stochastic energy losses. In order to confirm this hypothesis, more specific investigation is needed.

The GZK signal events populate the EHE region and tend to be horizontal, as described in a previous section. This allows one to discriminate them from the background. The signal is also concentrated in the deep part of the detector because of the more transparent ice there.

#### IV. SEARCH FOR EHE NEUTRINO SIGNAL

Using the empirical background model, the EHE signal search was performed based on the NPE and zenith angle information. The selection criteria are determined by using only MC data sets that are optimized with the observational data in the background dominated energy region ( $10^4 \leq \text{NPE} \leq 10^5$ ), following a blind analysis procedure.

It is found that the large spread of mis-reconstructed events extended to the signal region. We found that the angular resolution is related to the CoGZ position. Events whose CoGZs are at the bottom of the detector ( $\text{CoGZ} < -250$  m) and which pass through the edge or outside of the bottom detector are significantly mis-reconstructed horizontal. When an inclined track reaches at the edge of the bottom part of the detector, there is no more detector below, so that the hit timing pattern resembles a horizontal track. The very clean ice at the bottom part of the detector and the biggest dust layer at middle enhance this effect. Therefore, the data sample is divided into two by the CoGZ position as follows.

- region A:  $-250 < \text{CoGZ} < -50$  m, and  $\text{CoGZ} > 50$  m
- region B:  $\text{CoGZ} < -250$  m, and  $-50 < \text{CoGZ} < 50$  m

A clear difference between the backgrounds and the signal is seen in the zenith angle and total NPE relations as shown in Fig. 2. The atmospheric background muon distribution shows a steep fall in NPE and peaks in the vertical direction, while the GZK signal is mainly horizontal and at higher NPE, allowing the discrimination of the backgrounds by rejecting low NPE events and vertically reconstructed events. It is also obvious that the large spread in zenith angle direction for region B due to mis-reconstructed events.

The selection criteria to separate signal from background are determined for region A and B separately. The criteria are determined at first for each zenith angle bins, requiring the background level to be negligible compared to the signal ( $10^{-4}$  events per 0.1  $\cos(\text{zenith angle})$  bin per 242.1 days). After the optimization for each zenith angle bin, the determined cut-offs in NPE are connected with contiguous lines as shown in Fig. 2.

The expected numbers of signal and background events with the selection criteria are summarized in Table I.

TABLE I  
EXPECTED EVENT NUMBER

Models	Expected events in 242.1 days
GZK1 [4]	$0.16 \pm 0.00$ (stat.) $^{+0.03}_{-0.05}$ (sys.)
Atm. muon	$(6.3 \pm 1.4$ (stat.) $^{+6.4}_{-3.9}$ (sys.)) $\times 10^{-4}$

The effective area for each neutrino flavor averaged over all solid angles with the selection criteria is shown in Fig. 3.

#### V. RESULTS

The EHE neutrinos are searched for by applying the selection criteria determined in the previous section to the 242.1 days of observed data taken in 2007.

Since no event is found after the search, a 90 % C.L. upper limit for all neutrino flavors (assuming full mixing neutrino oscillations) is placed with the quasi-differential method based on the flux per energy decade ( $\Delta \log_{10} E = 1.0$ ) described in Ref. [9]. A 90 % C.L. preliminary upper limit for an  $E^{-2}$  spectrum is also derived as  $E^2 \phi_{\nu_e + \nu_\mu + \nu_\tau} \leq 5.6 \times 10^{-7} \text{ GeV cm}^{-2} \text{ s}^{-1}$

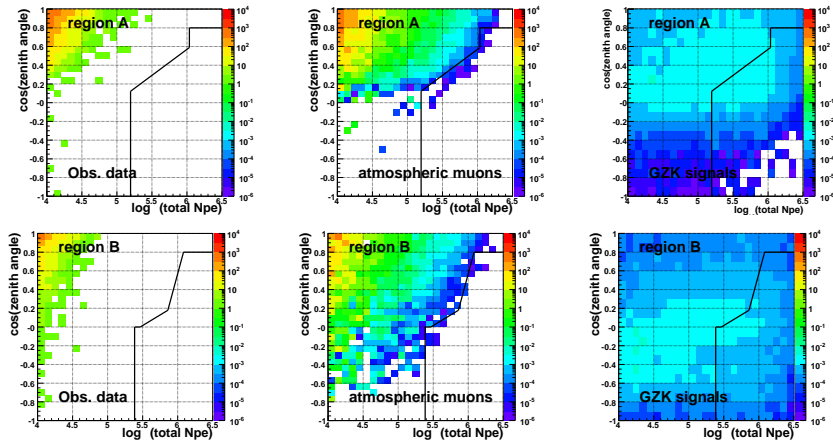


Fig. 2. The zenith angle Vs total NPE. The top plots are for region A and the bottom ones for region B. The plots are for the observational data, the background from the empirical model and the GZK signal[4] from left.

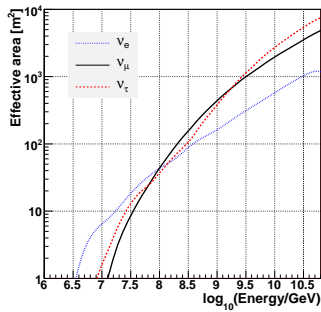


Fig. 3. The effective area for each flavor neutrino after applying the signal selection criteria averaged over all solid angles. Blue dotted line represents  $\nu_e$ , black solid line for  $\nu_\mu$  and red dashed line for  $\nu_\tau$ .

$\text{sr}^{-1}$ , where 90 % of the events are in the energy range of  $10^{7.5} < E_\nu < 10^{10.6}$  GeV, taking the systematics into account. These preliminary limits as well as results of several model tests are shown in Fig. 4. The derived limit is comparable to the Auger [13] and HiRes [16] limit. The AMANDA limit [12] for an  $E^{-2}$  flux is better than the limit by this analysis. This is because AMANDA has a better sensitivity for lower energy and the livetime is about twice as much as this analysis.

The systematics such as detector sensitivity, neutrino cross-section, hadronic interaction model, yearly variation are currently being investigated. The biggest uncertainty comes from the NPE difference observed by the absolutely calibrated light source in situ, and it is estimated to be on the order of 30 %. These systematics are included in the upper limit calculation. The details of the systematics estimation as well as more detail of this analysis will be presented in another paper in preparation.

#### ACKNOWLEDGEMENTS

We acknowledge the U. S. National Science Foundation, and all the agencies to support the IceCube project. This analysis work is particularly supported by the Japan Society for the Promotion of Science.

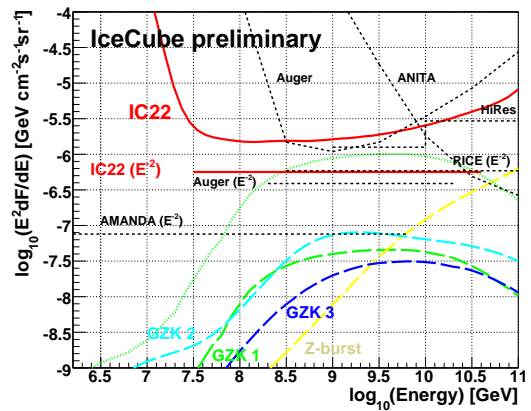


Fig. 4. The preliminary upper limit by the IC-22 EHE analysis (red solid) (all flavor) with the systematics taken into account. The thick long dashed green line represents GZK model 1 [4], light blue is for GZK model 2 [10], blue line is for GZK model 3 [17] and yellow for Z-burst model [11]. The dotted green line is 90 % C.L. upper limit for GZK model 1 by this analysis. The upper limit by other experiments are also shown with dashed lines [12], [13], [14], [15], [16]. Limits from other experiments are converted to all flavors where necessary assuming full mixing neutrino oscillations.

#### REFERENCES

- [1] The Pierre Auger Collaboration, *Science* **318**, 896 (2007).
- [2] V. S. Beresinsky and G. T. Zatsepin, *Phys. Lett.* **28B**, 423 (1969).
- [3] K. Greisen, *Phys. Rev. Lett.* **16**, 748 (1966); G. T. Zatsepin and V. A. Kuzmin, *Pisma Zh. Eksp. Teor. Fiz.* **4**, 114 (1966) [*JETP. Lett.* **4**, 78 (1966)].
- [4] S. Yoshida and M. Teshima, *Prog. Theor. Phys.* **89**, 833 (1993).
- [5] S. Yoshida *et al.*, *Phys. Rev. D* **69**, 103004 (2004).
- [6] T. K. Gaisser, *Cosmic Rays and Particle Physics* (Cambridge University Press, Cambridge, England, 1990) p206.
- [7] M. Nagano and A. A. Watson, *Rev. Mod. Phys.* **72**, 689 (2000).
- [8] D. Heck *et al.*, Report FZKA 6019, (Forschungszentrum Karlsruhe 1998).
- [9] X. Bertou *et al.*, *Astropart. Phys.*, **17**, 183 (2002).
- [10] O. E. Kalashev, V. A. Kuzmin, D. V. Semkoz, and G. Sigl, *Phys. Rev. D* **66** 063004 (2002).
- [11] S. Yoshida, G. Sigl and S. Lee, *Phys. Rev. Lett.* **81**, 5505 (1998).
- [12] Andrea Silvestri (IceCube), Proc. 31st ICRC (2009).
- [13] J. Abraham *et al.* (Auger), *Phys. Rev. Lett.* **100**, 21101 (2008).
- [14] P. W. Gohram *et al.* (ANITA), arXiv:0812.2715v1 (2008).
- [15] I. Kravchenko *et al.* (RICE), *Phys. Rev. D* **73**, 082002 (2006).
- [16] R. U. Abbasi *et al.* (HiRes), *ApJ* **684**, 790 (2008).
- [17] R. Engel *et al.*, *Phys. Rev. D* **64**, 093010 (2001)